A. Supplementary File

A.1. Acquisition of Fingerprint Images

The spectral power distribution in real-world fingerprint images shows remarkable difference with other real-world images which generally follow $1/f^{\alpha}$ distribution [1,3,4,7], where f represents the frequency and $\alpha \approx 2$. As can be observed from Fig. 3, the power distribution curve from the fingerprint images illustrates steep decline in lower frequency region and then it rapidly raises to reach its peak value, followed by its gradual decline.

Most energy from spectral power distribution in real-world fingerprint images is largely concentrated in the middle frequency bands. Therefore, it is necessary to perform additional experiments to evaluate the effectiveness of proposed method on detecting GAN-generated fake fingerprint images. Fig. A illustrates sample images from the test set for the performance evaluation and includes GAN-generated fake fingerprint images that are detected as real fingerprint images when subjected to proposed method.

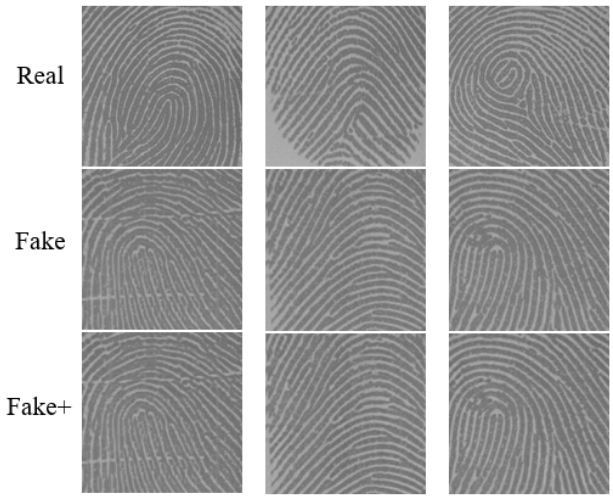

Figure A. Test image samples from real, fake and fake+ fingerprints.

A.2. Test Results from Spatial Domain Detector

This section provides additional results from the spatial domain fake image detector W [8] that were missed in the paper due to space constraints. Fig. B provides additional ROC plots by incorporating the proposed methods for detector W. These results illustrate consist decline in its detection performance although to a varying degree.

In Fig. Ba the performance of detector W drops notably more from the experiments where only PDC is employed, while in Fig. Bb, Fig. Bc, Fig. Be and Fig. Bf the drop-in performance from detector W is smaller when only using PDC. Since detector W is trained only using ProGAN and it shows great robustness for the ProGAN-generated images, the performance on ProGAN class images in test dataset is stable (almost no drop) as can be observed from the results in Fig. Bd.

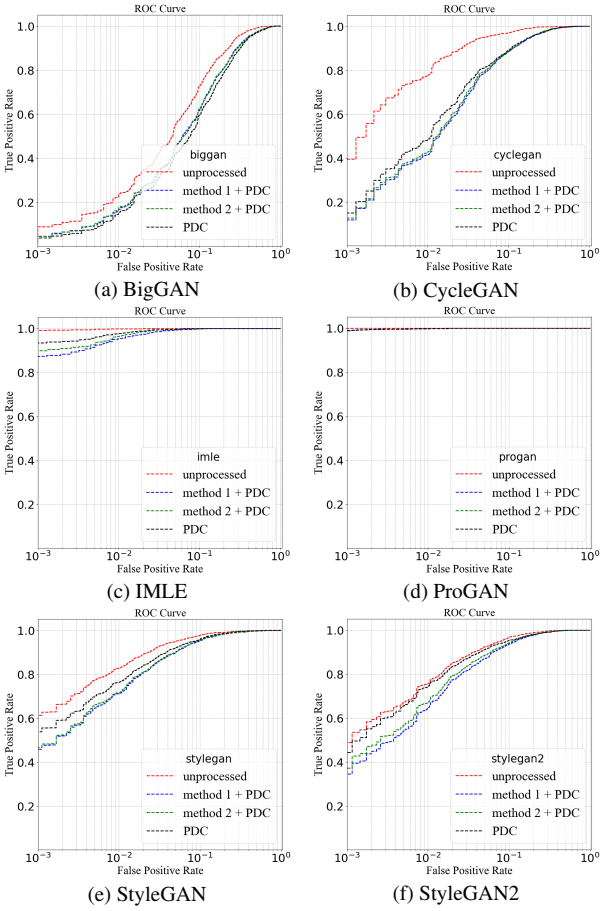

(a) BigGAN (b) CycleGAN (c) IMLE (d) ProGAN (e) StyleGAN (f) StyleGAN2

Figure B. ROC curves from the test results of proposed methods.

A.3. Implementation Details

Method 1 Implementation: The $\boldsymbol{l}_{mean}$ is estimated from all real-world images in the training dataset with the exclusion of fingerprint dataset, and we compute 1×128 size $\boldsymbol{l}_{mean}$ vector and $P(G(a))$ in Eq. (4) using Algorithm 1. For fingerprint images, we estimate its $\boldsymbol{l}_{mean}$ independently from respective database. We train nine SpectralGAN models for each class. For each model, the spectra of GAN-generated images of that class in training dataset are regarded as domain A and the spectra of real-world images of that class in training dataset are regarded as domain B.

For optimizing the SpectralGAN, we use Adam optimizer with initial learning rate of 0.0008 and linear descendant is adopted for learning rate decreasing policy. The training batch size is 2. We set $\lambda_1 = 10$ for L_{cyc} and $\lambda_2 = 5$ for L_{identity}. We observe that the training will collapse if L_{power} and L_{max} is introduced at the start of training

when the network is trained from scratch. To ensure stability during training, we activate power loss and max loss in 4000^{th} mini-batch and initialize $\lambda_3 = 8$ for L_{power} and $\lambda_4 = 5$ for L_{max}. We keep the same learning rate for the first 10000 mini-batches and linearly decay the rate to zero over the next 30000 mini-batches. Experiments in this paper are performed on a server running Ubuntu 18.04, with 64 GB RAM, an Intel i9-7900X, and three Nvidia GTX 1080ti. Once the model is trained, respective model is used for enhancing the corresponding class of the GAN-generated images and we use the enhanced images (Fake+) to compromise the detectors and evaluate the performance of proposed methods.

Method 2 Implementation: We use Algorithm 2 and estimate nine spectrum difference matrices $\Delta_1, \Delta_2 \ldots \Delta_9$ for nine classes in training dataset. Then each spectrum of GAN-generated test images in the corresponding class is subtracted by Δ_i.

PDC Implementation: We randomly select 100k, 200k and 500k of 1000 classes in ImageNet2012 images to build the respective power dictionary. The images from ImageNet2012 are resized to 256×256 pixels. For experiments on fingerprint dataset, we construct another power dictionary using FVC2002 [5], FVC2004 [6] and FVC2006 [2] dataset by excluding the synthetic fingerprint images.

Once the power dictionaries are constructed, spectra of input images are corrected using Algorithm 3. The test results presented in Tabs. 1 to 3 and Fig. 5 use the power dictionary constructed using 500k real images. As shown in Fig. 2, IDFT is finally used for transferring the processed spectra of GAN-generated images into the Fake+ images. The partition of dataset for training and testing images is detailed in Tab. I.

	Training		Testing	
	Real	Fake	Real	Fake
BigGAN	6400	6400	1600	1600
CRN	5105	5105	1277	1277
CycleGAN	8000	8000	2000	2000
IMLE	5105	5105	1277	1277
ProGAN	24000	24000	6000	6000
StarGAN	8000	8000	2000	2000
StyleGAN	12800	12800	3200	3200
StyleGAN2	12800	12800	3200	3200
Fingerprint	6912	5916	1728	1480

Table I. Dataset Organization

A.4. Difference of Spectrum

Fig. D presents 3D visualization of average differences Δ_i between real spectra and fake spectra from the images in training dataset of nine classes of images (Tab. I). These differences Δ_i are used in the spectrum difference normalization (Method 2) following Algorithm 2. As we observe from these figures, it is necessary to consider fake images from 9 classes differently, following Method 2, since Δ_i notably varies between these classes.

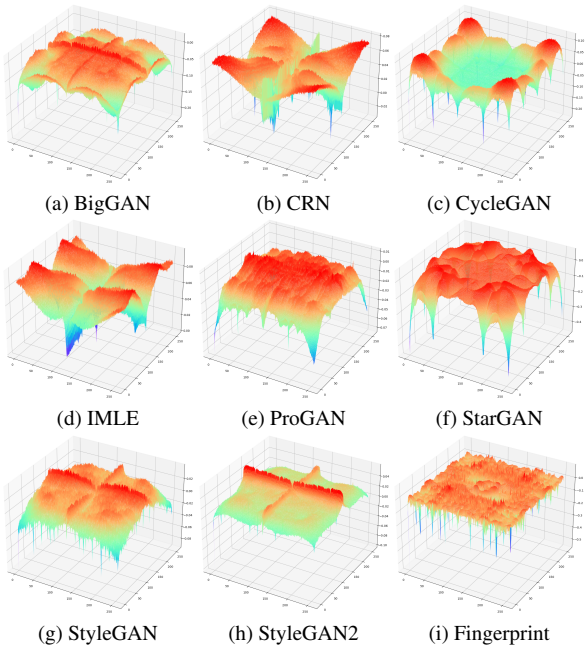

(a) BigGAN (b) CRN (c) CycleGAN

(d) IMLE (e) ProGAN (f) StarGAN

(g) StyleGAN (h) StyleGAN2 (i) Fingerprint

Figure D. Average spectrum difference between real images and GAN-generated images.

A.5. Average Spectrum

Fig. E presents the average spectrum of GAN-generated fake images and real-world images in training dataset of nine classes of images.

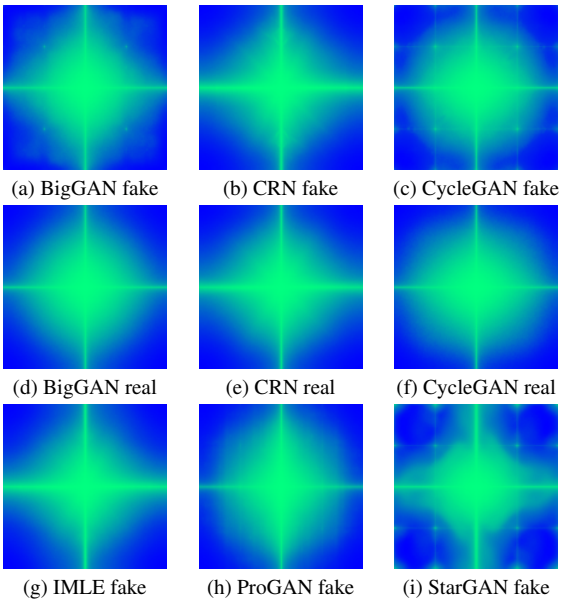

(a) BigGAN fake (b) CRN fake (c) CycleGAN fake

(d) BigGAN real (e) CRN real (f) CycleGAN real

(g) IMLE fake (h) ProGAN fake (i) StarGAN fake

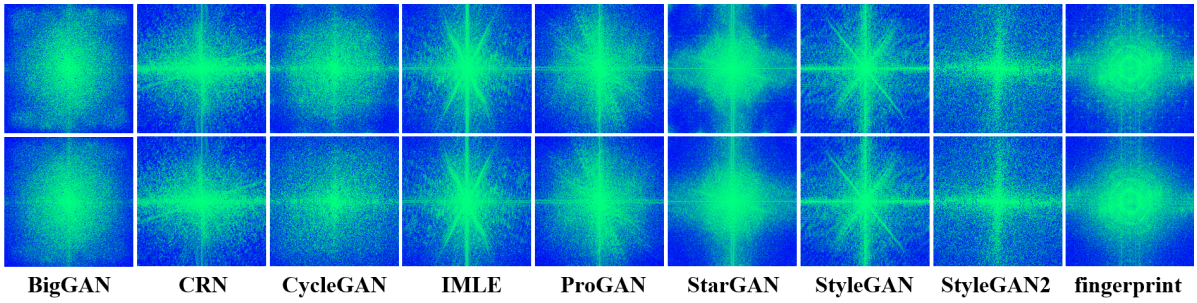

(a) Method 1 + PDC

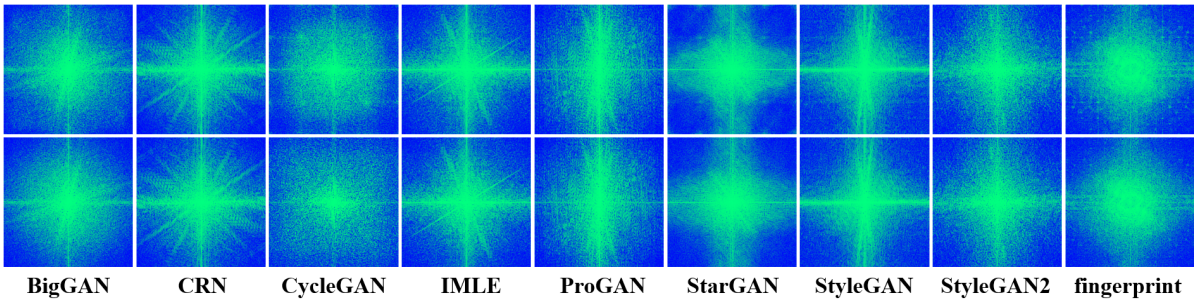

(b) Method 2 + PDC

Figure C. Examples of spectrum (first row) whose artifact patterns are successfully mitigated (second row).

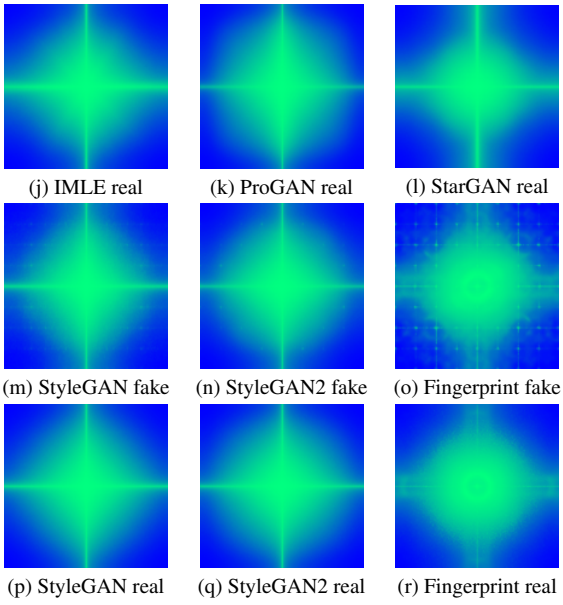

(j) IMLE real (k) ProGAN real (l) StarGAN real

(m) StyleGAN fake (n) StyleGAN2 fake (o) Fingerprint fake

(p) StyleGAN real (q) StyleGAN2 real (r) Fingerprint real

Figure E. Average spectra of GAN-generated fake images and real-world images.

A.6. Successful Examples

The successful elimination of artifacts by Method 1 + PDC is shown in Fig. Ca, the successful elimination of artifacts by Method 2 + PDC is shown in Fig. Cb. The first row of Fig. Ca and Fig. Cb represents the spectra with artifacts and the second row of Fig. Ca and Fig. Cb represents the spectra whose artifacts are mitigated by the respective methods.

A.7. Comparison in Spatial-domain Images

In Fig. F, we present sample images to observe the difference between the enhanced images (Fake+) and the original fake images. The organization of different images in Figs. Fb to Fk follows the sequences illustrated in Fig. Fa.

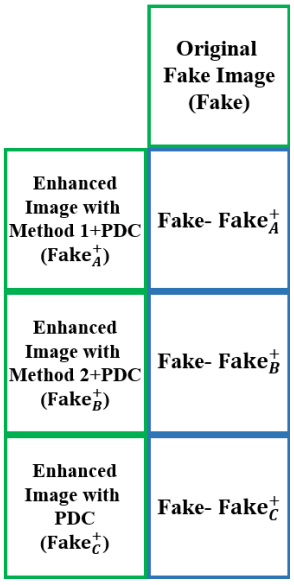

(a)

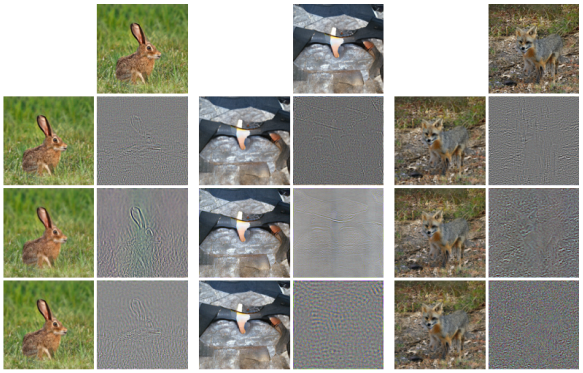

(b) BigGAN

(c) CRN

(d) CycleGAN

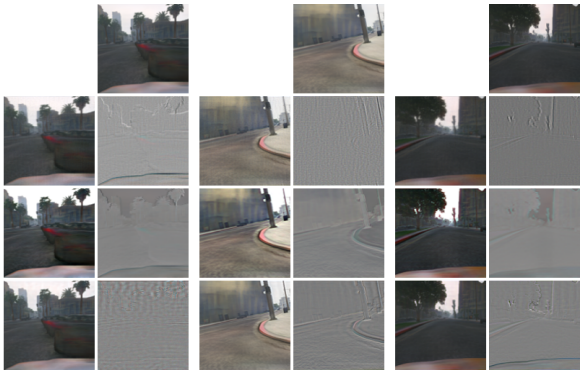

(e) IMLE

(f) ProGAN

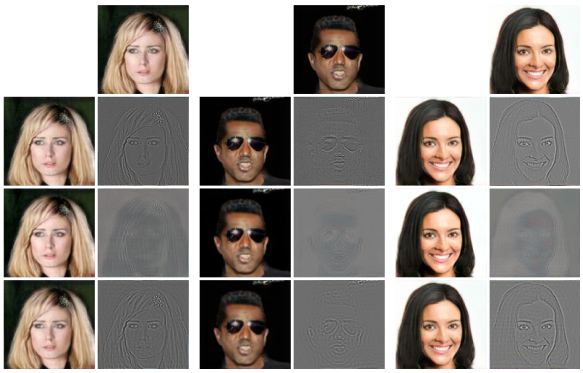

(g) StarGAN

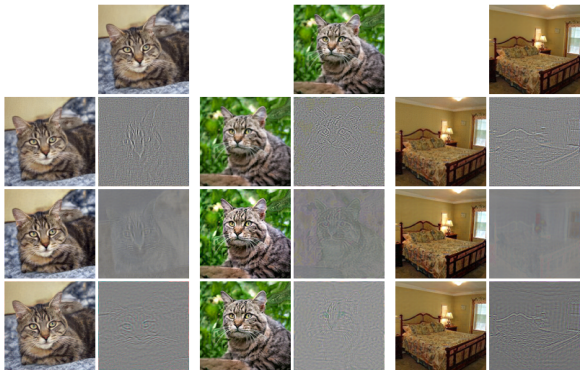

(h) StyleGAN

(i) StyleGAN2

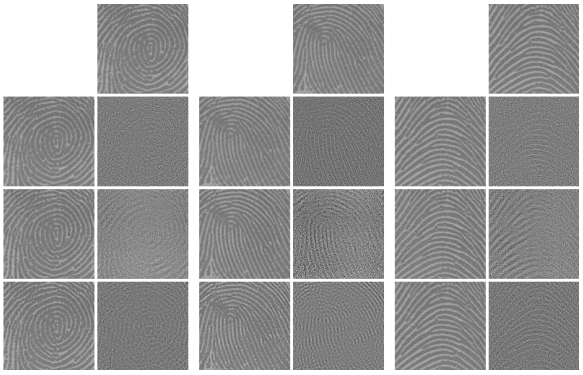

(j) Fingerprint

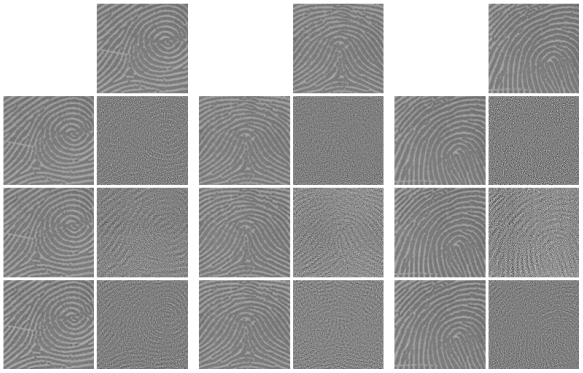

(k) Fingerprint

Figure F. Sample images to visualize imperceptible differences in the spatial domain using our methods.

References

[1] Geoffrey J Burton and Ian R Moorhead. Color and spatial structure in natural scenes. *Applied optics*, 26(1):157–170, 1987. 1

[2] Raffaele Cappelli, Matteo Ferrara, Annalisa Franco, and Davide Maltoni. Fingerprint verification competition 2006. *Biometric Technology Today*, 15(7-8):7–9, 2007. 2

[3] David J Field. Relations between the statistics of natural images and the response properties of cortical cells. *Josa a*, 4(12):2379–2394, 1987. 1

[4] David J Field. Wavelets, vision and the statistics of natural scenes. *Philosophical Transactions of the Royal Society of London. Series A: Mathematical, Physical and Engineering Sciences*, 357(1760):2527–2542, 1999. 1

[5] D. Maio, D. Maltoni, R. Cappelli, J.L. Wayman, and A.K. Jain. Fvc2002: Second fingerprint verification competition. In *2002 International Conference on Pattern Recognition*, volume 3, pages 811–814 vol.3, 2002. 2

[6] Dario Maio, Davide Maltoni, Raffaele Cappelli, Jim L Wayman, and Anil K Jain. Fvc2004: Third fingerprint verification competition. In *International conference on biometric authentication*, pages 1–7. Springer, 2004. 2

[7] DJ Tolhurst, Y_ Tadmor, and Tang Chao. Amplitude spectra of natural images. *Ophthalmic and Physiological Optics*, 12(2):229–232, 1992. 1

[8] Sheng-Yu Wang, Oliver Wang, Richard Zhang, Andrew Owens, and Alexei A Efros. Cnn-generated images are surprisingly easy to spot... for now. In *Proceedings of the IEEE/CVF Conference on Computer Vision and Pattern Recognition*, pages 8695–8704, 2020. 1